

Supporting Information

Improved enantioselectivity in thiol-ene photopolymerization of Sulphur-containing polymers with circularly polarized luminescence

Chen-Lu He, Zeyu Feng, Yan Li, Manman Zhou, Liyang Zhao, Sizhen Shan, Mengqiao Wang, Xin Chen*, Xi-Sheng Wang*, Gang Zou*

Experimental Procedures

Materials.

Racemic 3-methyl-2-butanethiol, 1-phenylethanethiol, N-Vinylacetamide were purchased from Alfa Aesar Company. Other compounds and all solvents were obtained from Sinopharm. Co. Ltd., and were purified by standard procedures before use. 1-phenylethanethiol-d were prepared according to literatures^[1]; the isotopic purity is > 75%.

CPL-triggered asymmetric thiol-ene click reaction.

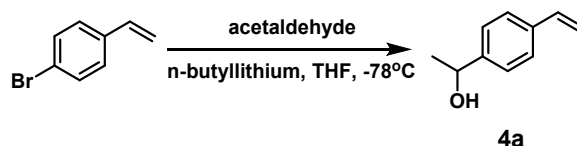
The 10 mW/cm² CPL (250-350nm), generated by Babinet-Soleil prism from ultra-high pressure mercury lamp, was used for enantioselective thiol-ene click reaction. Racemic thiols (0.5 mmol), activate enes (0.5 mmol) and 1,4-cyclohexadiene (0.25 mmol) were dissolved in acetonitrile (1 mL) and put into a quartz cuvette. Then above solutions were subjected to CPL irradiation for a period of time.

CPL-triggered asymmetric thiol-ene photopolymerization

As for photopolymerization without addition of HAD, the monomer **4c** (32.8mg, 0.2mmol) was dissolved in acetonitrile (1mL) and put into a quartz cuvette. As for photopolymerization with addition of HAD, extra HAD (8mg, 0.1mmol) was added in the quartz cuvette. Then above solutions were subjected to CPL (L-CPL or R-CPL) irradiation. After photopolymerization, the polymerization solution was precipitated into a large amount of n-hexane, collected by centrifugation, and dried in vacuum at room temperature overnight, afford poly(thioether) as a white solid.

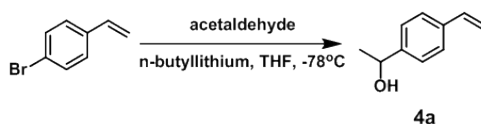
Instruments.

¹H NMR were recorded on Bruker Avance 400 MHz. CD and UV-vis spectra were obtained in a 1.0 mm quartz cell at 25 °C using a JASCO CD spectrometer J-810 and Shimadzu UV-2550 PC spectrophotometer, respectively. The specific rotation data was obtained from Anton Paar MCP 100. HPLC were performed on a column of Chiralpak (Daicel Chemical Industries Ltd.) using isopropanol in n-hexane solution (5/95, v/v). Size exclusion chromatography (SEC) was performed in THF (0.2 mg/mL) at a flow rate of 0.3 mL/min on Jasco Pu-418 pump liquid chromatograph equipped with Jasco UV-4070 and CD-4095 detectors (set at 40 °C), using a series of two linear TSK gel GMHHR-H columns. Molecular weight (Mn) and its distribution (Mw/Mn) were reported relative to polystyrene standards. Circularly polarized fluorescence was measured using a JASCO CPL-300 spectrometer. Dynamic light scattering (DLS) was recorded using an ALV/CGS-3 compact goniometer system. Cryo-electron microscopy characterization was performed on a Tecnai F20.



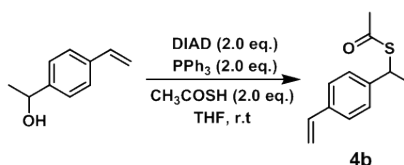
Synthesis of racemic 1-(4-vinylphenyl) ethane-1-thiol (4-VPET) monomer

(1) Preparation of racemic 1-(4-vinylphenyl)ethanol **4a**



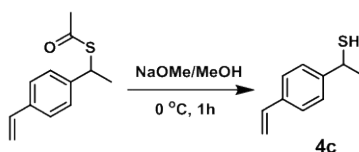
A solution of 910 mg of 4-bromostyrene in 25 mL of dry THF was cooled to $-78\text{ }^{\circ}\text{C}$ and 2.3 mL, 2.4 M n-butyllithium was added. After 20 min at $-78\text{ }^{\circ}\text{C}$, a solution of 1.3 mL, 5.0 M acetaldehyde in THF was added dropwise. After the addition was complete, the solution was slowly warmed to room temperature, and stirred for 2 h. Then, water was added dropwise and the mixture was extracted into ethyl acetate. The combined organic layers were washed with saturated NaCl solution, dried over Na_2SO_4 , and then filtered. The filtrate was concentrated *in vacuo* and the desired product **4a** (607 mg) was obtained after purification by flash chromatography on silica gel. Yield: 82%. $^1\text{H NMR}$ (400 MHz, CDCl_3) δ 7.39 (d, $J = 7.9$ Hz, 2H), 7.32 (d, $J = 7.9$ Hz, 2H), 6.71 (dd, $J = 17.6$, 10.9 Hz, 1H), 5.74 (d, $J = 17.6$ Hz, 1H), 5.23 (d, $J = 10.9$ Hz, 1H), 4.88 (q, $J = 6.4$ Hz, 1H), 1.88 (s, 1H), 1.48 (d, $J = 6.4$ Hz, 3H).

(2) Preparation of corresponding thioester **4b** via the Mitsunobu protocol.



Diisopropyl azodicarboxylate (DIAD) (2.95 mL, 15.0 mmol) was added dropwise and *via* syringe to an ice-cooled solution of triphenylphosphine (3.93 g, 15.0 mmol) in dry THF (30 mL) under argon. After 1 h, a solution of the racemic 1-(4-vinylphenyl)ethanol (**4a**, 1.1 g, 7.50 mmol) and thioacetic acid (1.07 mL, 15.0 mmol) in THF (10 mL) was slowly injected and the mixture was stirred continuously while warming to room temperature. After 12 h, the solvent was evaporated *in vacuo*, the resulting yellow slurry was suspended in *n*-hexane (40 mL) and stirred for 6 h. After removal of the precipitate formed by filtration, the filtrate was concentrated *in vacuo* and the desired product **4b** (1.0g) obtained after purification by flash chromatography on silica gel. Yield: 71%. $^1\text{H NMR}$ (400 MHz, CDCl_3) δ 7.35 (d, $J = 8.1$ Hz, 2H), 7.29 (d, $J = 8.0$ Hz, 2H), 6.68 (dd, $J = 17.6$, 10.9 Hz, 1H), 5.72 (d, $J = 17.6$ Hz, 1H), 5.23 (d, $J = 10.9$ Hz, 1H), 4.73 (q, $J = 7.1$ Hz, 1H), 2.29 (s, 3H), 1.64 (d, $J = 7.2$ Hz, 3H). $^{13}\text{C NMR}$ (101 MHz, CDCl_3) δ 195.1, 142.3, 136.8, 136.4, 127.5, 126.5, 114.0, 42.8, 30.6, 22.2. *GCMS Calcd. for M^+ $\text{C}_{12}\text{H}_{14}\text{OS}$ 206, found 206.*

(3) Reduction of thioester **4b** to racemic 1-(4-vinylphenyl) ethane-1-thiol (4-VPET) monomer **4c**.



Sodium methoxide (NaOMe, 141 mg, 2.6 mmol) and anhydrous methanol (5 mL) were added to a dry Schlenk tube equipped with a stir bar. The reaction mixture was cooled to $0\text{ }^{\circ}\text{C}$, and corresponding thioester (**4b**, 208.3 mg, 1.01 mmol) was slowly added. After 1 h of stirring at $0\text{ }^{\circ}\text{C}$, the reaction was quenched with diluted hydrochloric acid solution (5%). The water layer was extracted with Et_2O (3 \times). The combined organic layers was washed with saturated NaCl solution and then dried over MgSO_4 . After filtration and evaporation, the desired product **4c** (122mg) obtained in excellent yield after purification by flash-chromatography on silica gel. Yield: 74%. $^1\text{H NMR}$ (400 MHz, CDCl_3) δ 7.37 (d, $J = 8.2$ Hz, 2H), 7.32 (d, $J = 8.2$ Hz, 2H), 6.69 (dd, $J = 17.6$, 10.9 Hz, 1H), 5.73 (d, $J = 17.6$ Hz, 1H), 5.23 (d, $J = 10.9$ Hz, 1H), 4.30 – 4.13 (m, 1H), 1.98 (d, $J = 5.1$ Hz, 1H), 1.66 (d, $J = 7.0$ Hz, 3H). $^{13}\text{C NMR}$ (101 MHz, CDCl_3) δ 145.6, 136.7, 136.5, 126.7, 126.6, 113.9, 38.6, 26.1. *GCMS Calcd. for M^+ $\text{C}_{10}\text{H}_{12}\text{S}$ 164, found 164.*

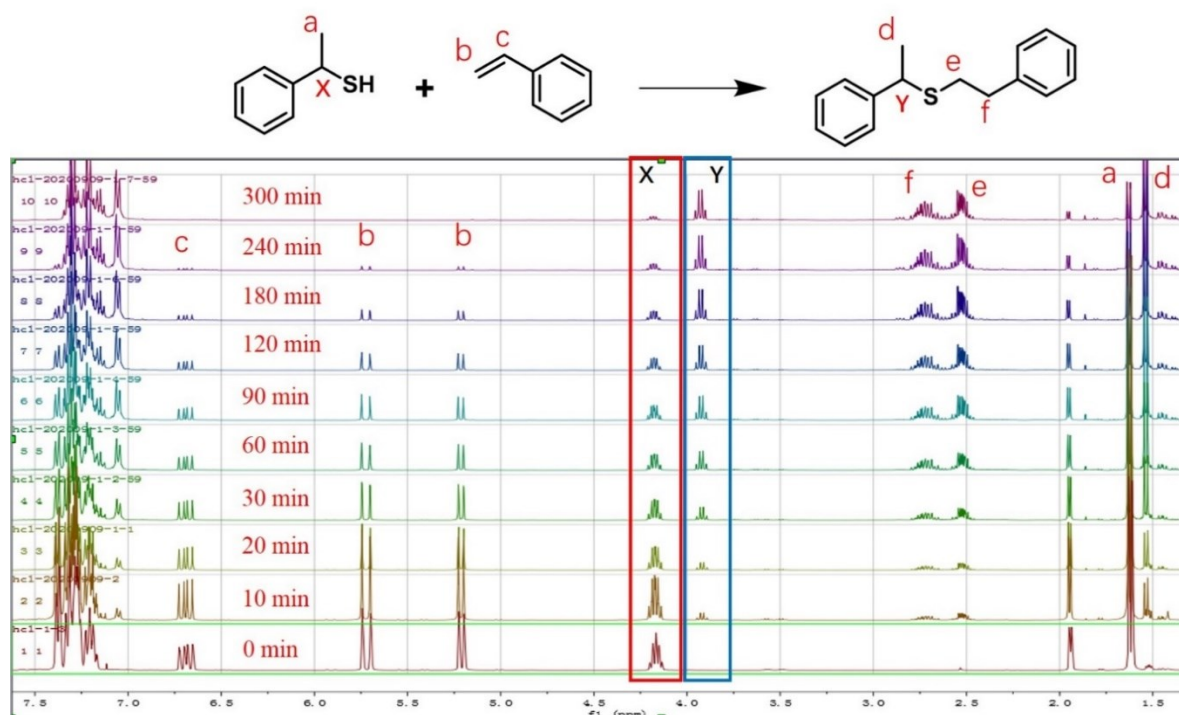


Figure S1. Reaction kinetics in bulk solution containing 1-phenylethanethiol and styrene in CDCl_3 measured by ^1H NMR. The sample was exposed to CPL for specific time intervals (0, 10, 20, 30, 60, 90, 120, 180, 240 and 300 min) prior to each ^1H NMR measurement.

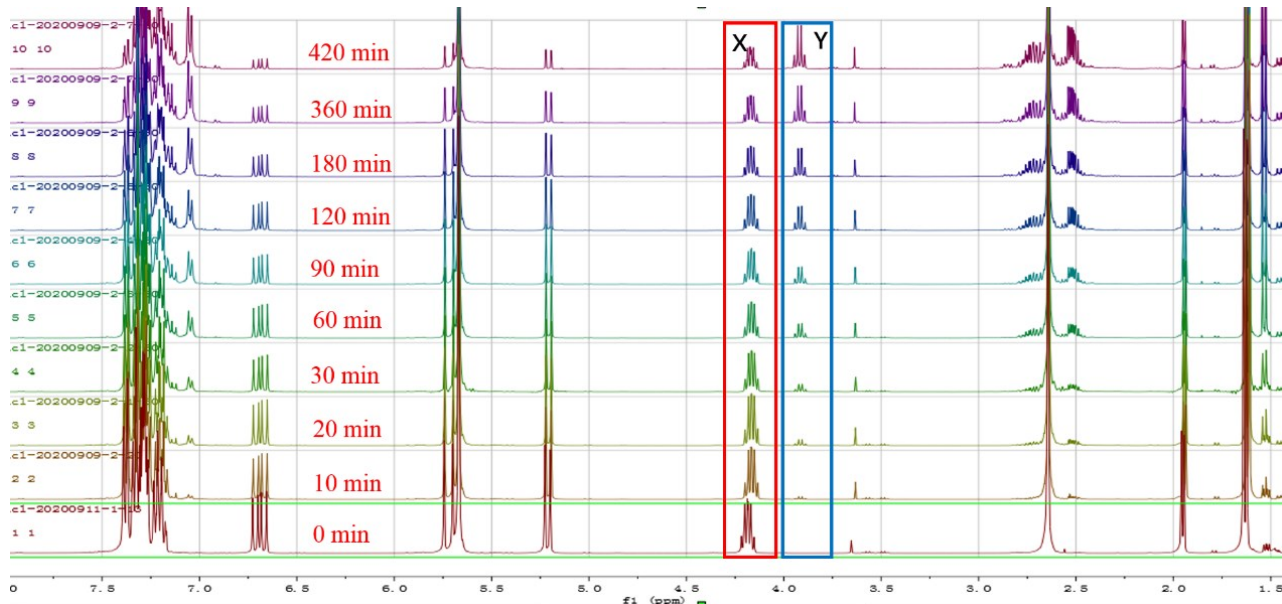
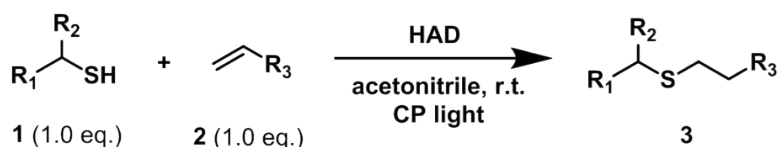
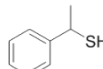
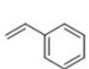
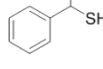
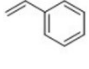
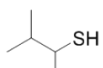
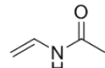
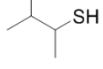
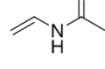
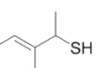
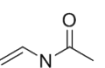
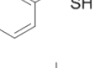
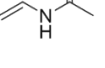
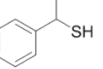
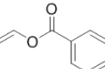
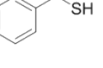
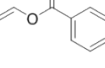


Figure S2. Reaction kinetics in bulk solution containing 1-phenylethanethiol, styrene and HAD in CDCl_3 measured by ^1H NMR. The sample was exposed to CPL for specific time intervals (0, 10, 20, 30, 60, 90, 120, 180, 360 and 420 min) prior to each ^1H NMR measurement.

Table S1. Evaluation of substrate scope of racemic thiols and activate enes with/without addition of HAD.

Entry	thiol.	ene.	HAD (eq.)	Time (h)	Conv. (%)	Product	ee (%)
1			-	2	52	(3a)	2.8
2			0.5	7	51		4.0
3			-	2.5	51	(3b)	1.5
4			0.5	7.5	52		2.0
5			-	2	47	(3c)	2.2
6			0.5	7	51		4.1
7			-	2	49	(3d)	2.1
8			0.5	7	50		3.9

1 (0.5 mmol), **2** (0.5 mmol) were stirred in acetonitrile (1 mL) at room temperature. The ees (error < 2%) were determined by chiral HPLC.

According to various thiols, the differences in steric hindrance between alkyl groups is smaller than that between aryl and alkyl groups. The reaction rate of thiols with alkyl group is slower than that with aryl group (entries 3 & 4, and entries 5 & 6, Table S1), because the thiols with aryl groups could absorb CPL better. After confirming the skeleton of thiols, we chose vinyl benzoate, N-vinylbenzamide and styrene as the acceptances of thiyl radical, since compared with electron-poor alkenes, electron-rich or -neutral alkenes match the thiyl radical, an electrophilic radical. Little differences could be observed, that implies the radical additions are similar. While considering the possibility of acyl exchange reaction to produce thioester, styrene-type alkene was selected to carry out the polymerization.

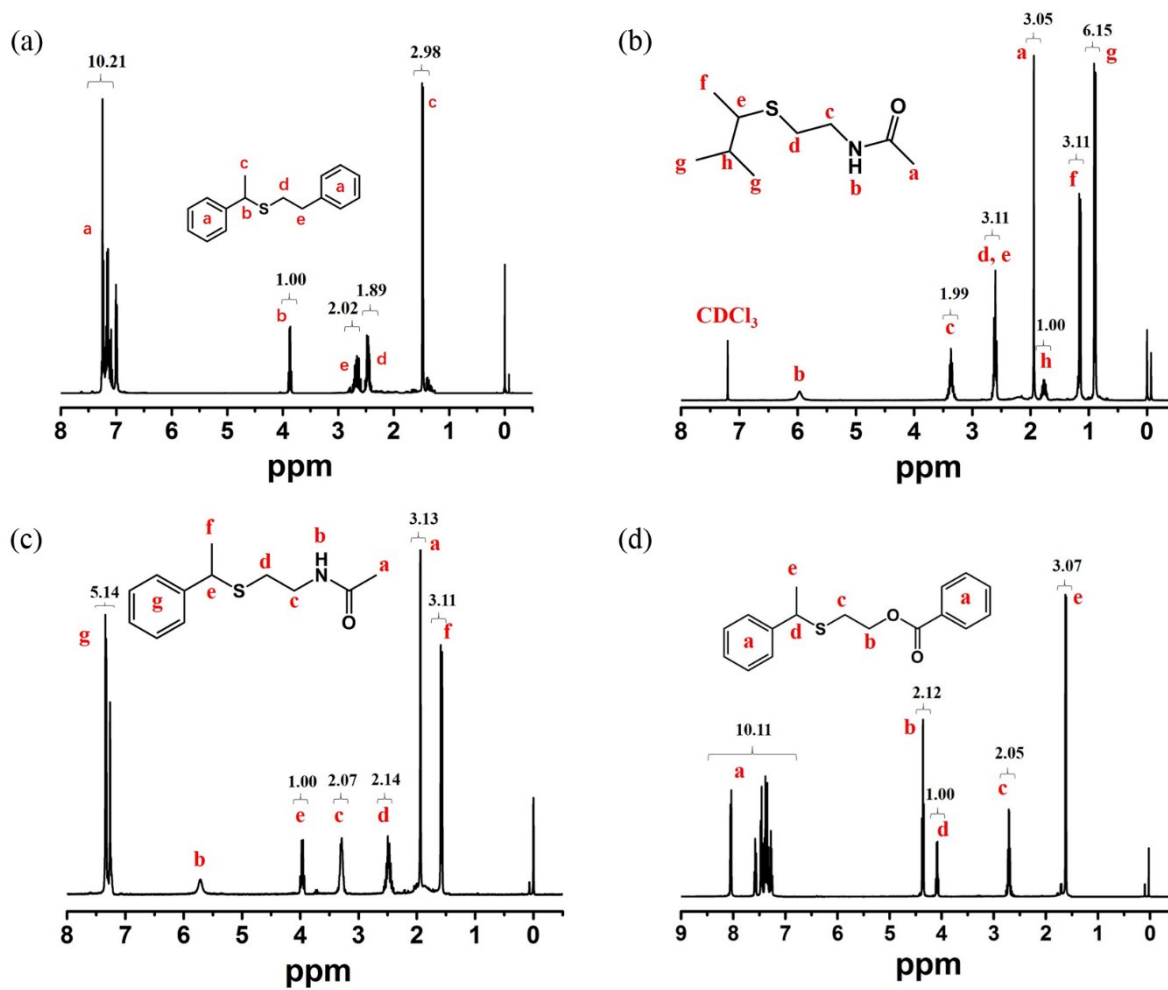


Figure S3. Molecular structure and the ^1H NMR spectra of addition product (a) **3a**, (b) **3b**, (c) **3c** and (d) **3d**.

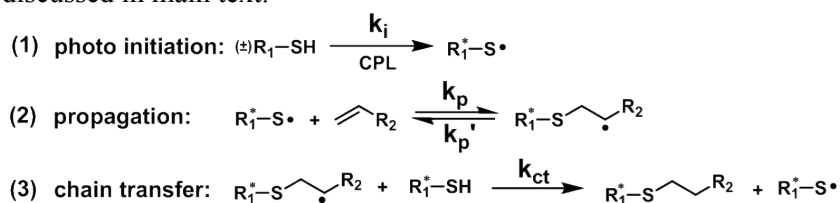
The thiol-ene reaction kinetics.

The reaction kinetics of thiol-ene reaction has been extensively investigated in many literature studies. All previous analysis, to the best of our knowledge, have ignored how the reaction kinetics could influence the ee of the final product. The overall framework of our model is similar to the previous ones, with more details and elementary reactions now included to account for two critically important features in our reaction system, enantioselectivity and additional HAD.

First, Eq1. is the photo initiation step. Note that in our system the thiol reactant itself acts as the photo initiator, whereas in some literature studies additional photo initiators were used and the photolysis of thiol was often ignored in those cases. Important, this is the only elementary reaction where any asymmetric force is introduced, and therefore serves as the ultimate source of enantioselectivity of the whole reaction system.

Eq2 and Eq3 make up the two legs of the characteristic cycle of thiol-ene chemistry. They describe, respectively, the propagation step in which thiyl turns into a carbon-centered radical, and the chain transfer reaction, in which the carbon-centered radicals react with another thiol to “regenerate” a thiyl radical. Herein, we have to take stereochemistry into consideration. The only chiral species in Eq2 is the thiyl radical. Thus, the same k value can be assumed for both thiyl enantiomers since the thiyl-ene coupling will not introduce any new chiral center in our systems with styrene and a few other enes used in this study. (This not generally true with some other more complicated enes).

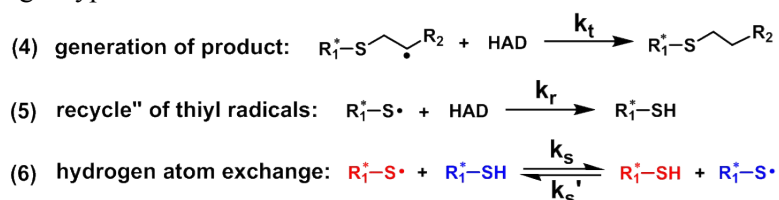
On the other hand, both the carbon-centered radical and thiol in Eq3 contain one chiral center, resulting four possible enantiomeric and/or diastereomeric combinations. To fully describe this reaction, three k values are needed (since two of the four cases should have the exactly same k value due to the symmetry.) In the small molecule case like styrene, we assume that all the k values are the same. This is a reasonable approximation because the two chiral centers are far away from each other. This assumption does not hold anymore in case of polymerization, as briefly discussed in main text.



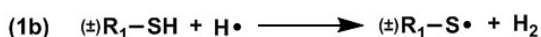
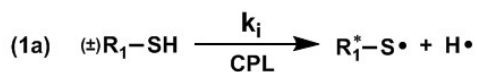
The above reactions are virtually the same as in previous kinetics models. The following few reactions are more unique to our systems.

Additional HAD can donate a hydrogen atom to either the carbon-centered radical or the thiyl radical, and this is modeled using Eq4 and Eq5, respectively. The consequence of these two reaction are drastically different. While Eq4 simply generates the final product, Eq5 effectively “recycle” the thiyl radicals back to thiol molecule, the starting material. As elaborated later, this is key elementary reaction step responsible for the enhanced enantioselectivity in our system. Conveniently, both Eq4 and Eq5 need one k value only since HAD we used in this study is achiral.

Eq6 describes the hydrogen atom exchange between of thiyl and thiol. This reaction had been completely ignored in previous studies because it would produce no net results when stereochemistry was not a concern. However, in our system, this self-scrambling could affect the final ee, for instance, when a left-type thiyl radical reacts with a right-type thiol molecule.



There is another mechanism might also contribute to the dual effect of HAD, i.e., lowered reactivity and enhanced enantioselectivity. While a thiyl radical with chiral preference is produced in the CPL-induced photolysis (eq1), the other product of is probably a H radical (eq1a). Such a H radical should be highly reactive. Without additional HAD, one possible fate of the H radical is to react with hydrogen from another thiol molecule (eq1b). This would generate another thiyl radical, which will continue further along the reaction route starting from eq2. This alternative route must carry no chiral preference and therefore ultimately contribute negatively to the overall enantioselectivity. With HAD, however, most active H radicals should be quickly trapped and this terminates the alternate reaction route. This mechanism should also lower the overall rate of the thiol-ene reaction but promote its enantioselectivity by selectively slowing down the non-enantioselective route.



This set of the differential equations has no analytical solution in closed form, but can be numerally simulated through step integrations. A set of simulation results is presented in Figure S4, it is intermediately clear that adding HAD has two important consequences: suppressed reactivity and enhanced enantioselectivity. These two effects are strongly interrelated. By examining scheme S1, one can easily see how additional HAD slows down the reaction, since it opens a new pathway for thiyl radical to return to the starting material. Unsurprisingly, a greater stoichiometric amount of HAD results in slower reaction rate, as shown in Figure S4a. The actual dependence of the reaction rate on the ratio of HAD: thiol is quite complicated because HAD could also affect the production rate of the final products through step 4 (Eq4).

The effect of HAD on enantioselectivity is less straightforward. A close analysis of the kinetics model reveals that there are two pathways of thiyl radicals: one is “physical”, generated from photolysis with CPL, and the other is “chemical”, produced from hydrogen abstraction from thiol by other radicals (either carbon-centered radicals (eq3) or other thiyl radicals (Eq6)). Although each thiyl radical is indiscriminable with each other, the two populations carry very different enantioselectivity. At the very beginning of the reaction process, this only source of thiyl radicals is photolysis of thiol molecule, which is initially racemic. This should generate a steady stream of thiyl with a fixed ee, determined only by difference in absorption coefficients of the two thiol enantiomers (about 8.0% under our experimental condition). This sets the up limit of ee one can obtain in this reaction system. As the reaction proceeds, concentration of thiyl radicals builds up quickly and the absolute rate of hydrogen abstraction reaction with thiol becomes comparable with photolysis. This period of time required to accumulate a significant concentration of thiyl radicals is the characteristic induction period in thiol-ene kinetics. It typically corresponds to a very small extent of reaction (ee < 4%) and lasts a few to tens of minutes under our experimental conditions. Important, the thiyl radicals initially generated “chemically” from thiol carry no enantioselectivity since thiol remains largely racemic and the hydrogen abstraction process virtually does not differentiate stereochemistry. Therefore, the overall ee of thiyl radicals drops very quickly due to “dilution” of the high ee thiyl population from photolysis with the low-to-none ee population generated through hydrogen abstraction.

With the reaction proceeding further, the kinetics enters a period of “steady state” where the thiyl radical concentrations remain significant but decrease steadily because of gradual consumption of reactants. As shown in Figure S4b, the ee value enters a tilted plateau: it is largely flat and decreases steadily but very slowly, at a much slower rate than in the induction period. This decrease can be attributed to differential consumption of the two enantiomers in thiol: the more reactive enantiomer always consumes faster, effectively enriching the relative concentration of the other. This effect is small but accumulative since it always contributes negatively to overall enantioselectivity, and it applies to both the “physical” and “chemical” pathways, making the former less enantioselective and latter slightly more anti-enantioselective (always opposite with the ee of the former). As the consequence, the overall ee decrease steadily and continuously with reaction gradually approaching completion, just as our model predicts.

Adding HAD will strongly influence the process of accumulation of thiyl radicals by opening up a new pathway to “destruct” them and turning them back into thiol molecule. This lowers the “stead state” concentration of thiyl radicals, and effectively shortens the induction period (in the extent of reaction not in absolute reaction time). As seen in Figure S4b, ee reached the plateau early and earlier plateau corresponds the higher altitude in term of the absolute ee value. This agrees very well with our experimental results: much higher ee was observed with a greater amount of HAD relative to thiol by sacrificing reactivity.

The two effects of additional HAD, improved enantioselectivity and suppressed reactivity, can also be understood in a less quantitative but more intuitive way. In typical thio-ene reactions, thiol plays two very different roles, the source of thiyl (as in Eq1) and the donor of hydrogen atom (as in Eq3 and Eq4). Adding HAD opens a new pathway for thiyl radical to return to thiol. This not only slows down the reaction, but at the same time, it also “competes” with hydrogen abstraction from thiol molecule, the latter of which necessarily induces racemization (it is actually slightly worse than racemization due to the differential consumption of the more reactive enantiomer, as state earlier.). This process effectively “refreshes” the population of thiyl, causing a greater fraction of thiyl to be generated through photolysis by CPL which carries high ee. To summarize, adding extra HAD improves overall enantioselectivity by paying the price of lowered reactivity.

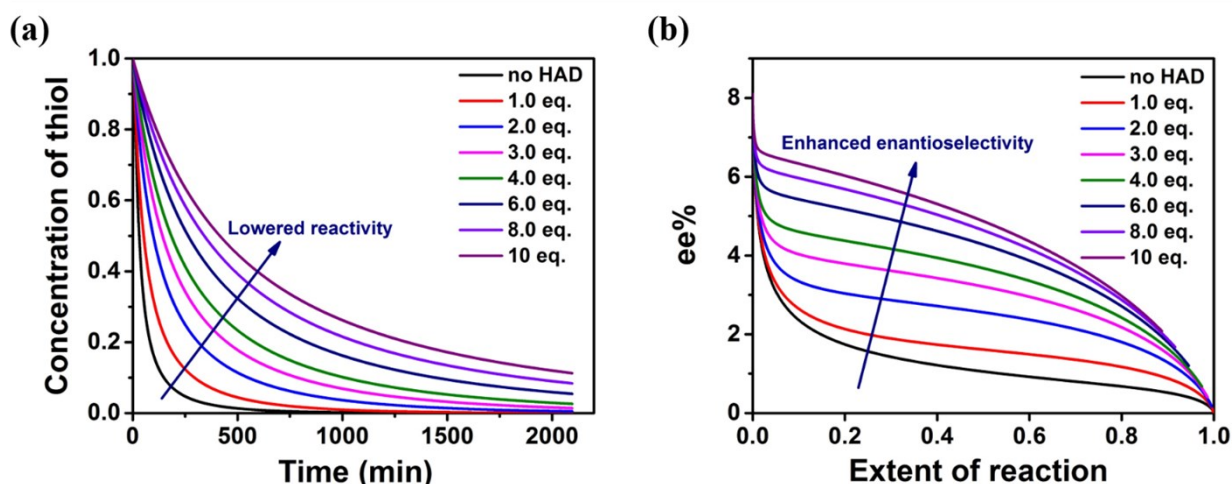


Figure S4. (a) Simulation of concentration of thiol as a function of exposure time upon without HAD or with different eq. HAD, respectively. (b) Simulation of ee values of product as a function of the extent of reaction upon without HAD or with different eq. HAD, respectively.

The reaction between racemic 1-phenylethanethiol-*d* and enes.

In order to further prove s the HAD could change the process of thiol-ene click reaction, racemic 1-phenylethanethiol-*d*^[1] was synthesized (75% purity) and reacted with N-vinylacetamide without or with addition of HAD, respectively. As for the reaction without the presence of HAD, 1-phenylethanethiol-*d* directly reacted with N-vinylacetamide and gave the final product **3d-d** (Figure S5a). Since one H atom at b position was substituted by D atom, the integrated intensity ratio at a and b positions of **3d-d** should be 1.0 in ¹H NMR. As expected, the integrated intensity ratio was measured to be about 1.3 (Figure S5b), a little higher than the theoretical values, which should be ascribed to the purity of 1-phenylethanethiol-*d* (75%). Upon the HAD was added to the reaction system, the integrated intensity ratio increased to 1.89 (Figure S5c), closely to the theoretical values for product **3d**. Above results confirmed that hydrogen atom of HAD really participated in thiol-ene click reaction.

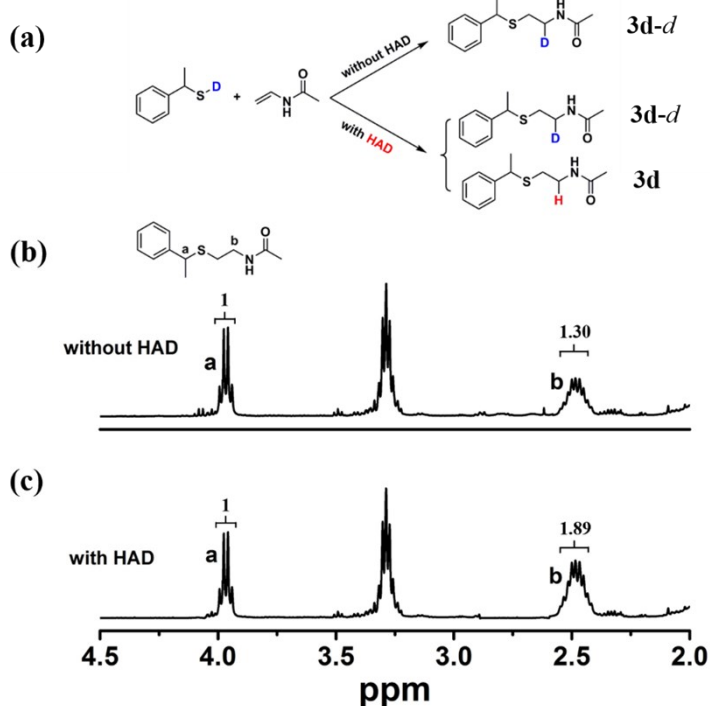


Figure. S5 (a) Reaction of 1-phenylethanethiol-*d* and N-Vinylacetamide without/with addition of HAD, respectively. ¹H NMR spectra of product **3d** (b) without and (c) with addition of HAD, respectively.

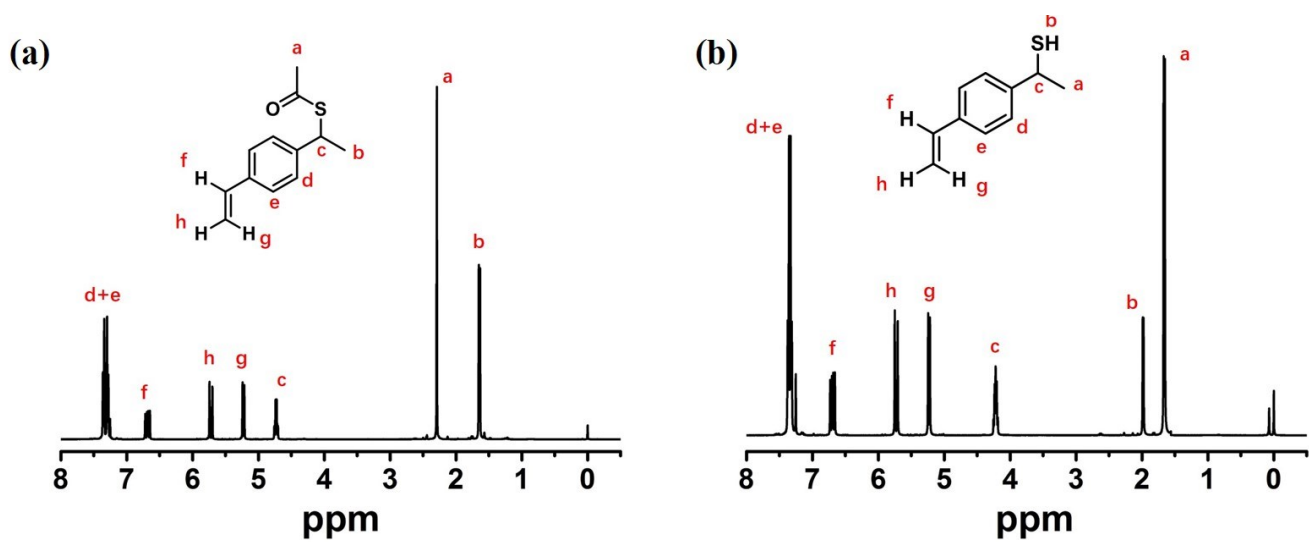


Figure S6. Molecular structure and ^1H NMR spectra of racemic compound (a) **4b** and (b) **4c**.

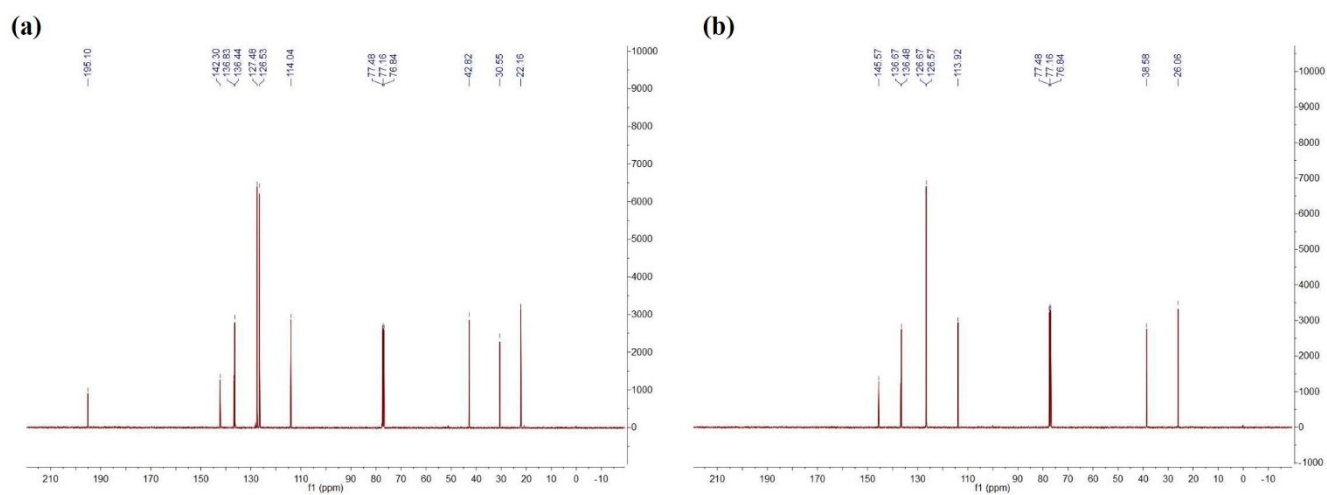


Figure S7. ^{13}C NMR spectra of racemic compound (a) **4b** and (b) **4c**.

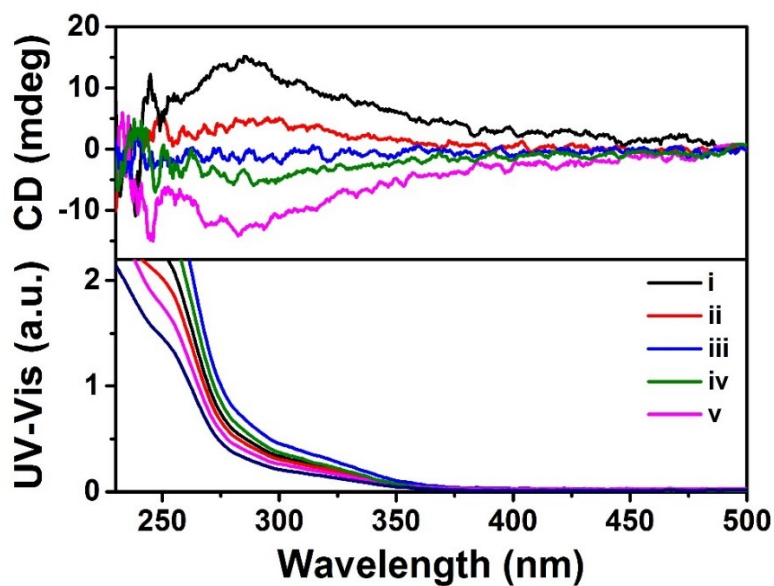


Figure S8. CD spectra of poly(thioether) (0.05 mg/mL in methanol) prepared using (i) R-CPL with additional HAD, (ii) R-CPL without HAD, (iii) unpolarized UV light, (iv) L-CPL without HAD and (v) L-CPL with additional HAD.

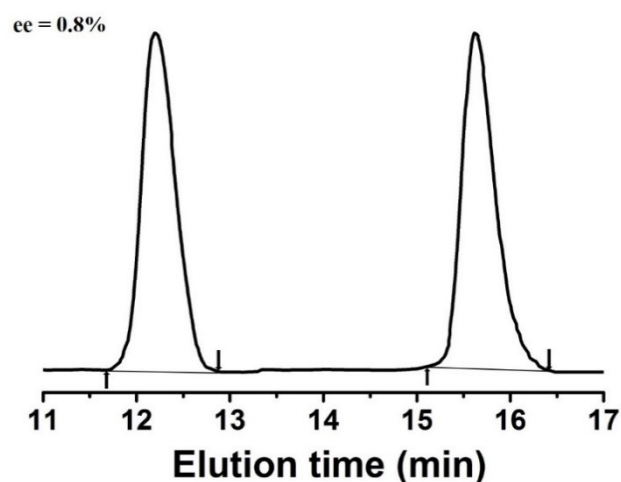


Figure S9. HPLC chromatograms of the residual reaction solution after unpolarized UV irradiation (containing unreacted 4-VPET monomer).

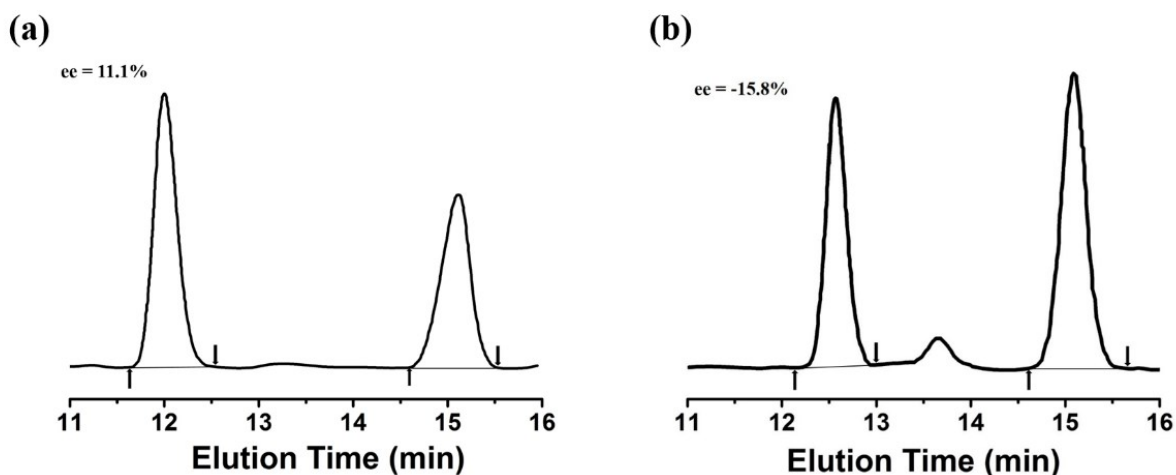


Figure S10. HPLC chromatograms of the residual reaction solution after (a) R-CPL and (b) L-CPL irradiation (containing unreacted 4-VPET monomer) without HAD.

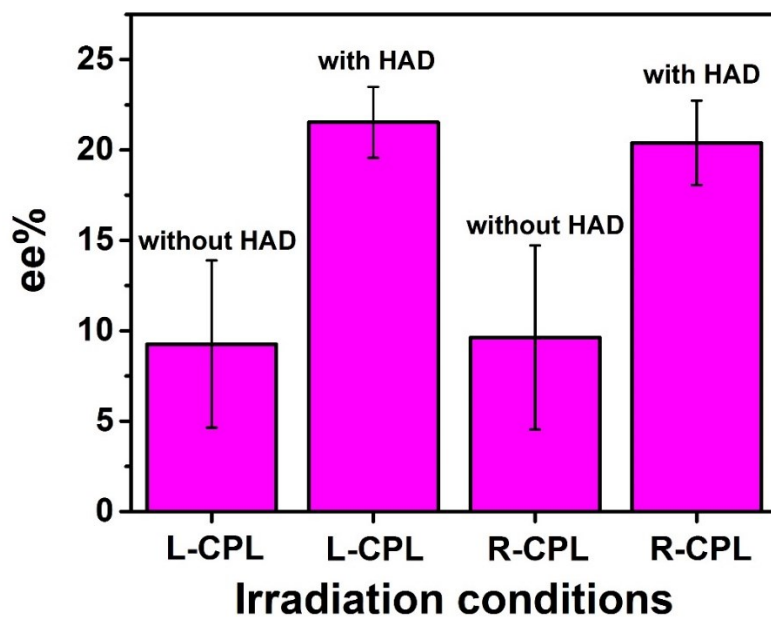


Figure S11. HPLC results of the residual reaction solutions after CPL irradiation without or with extra HAD, respectively.

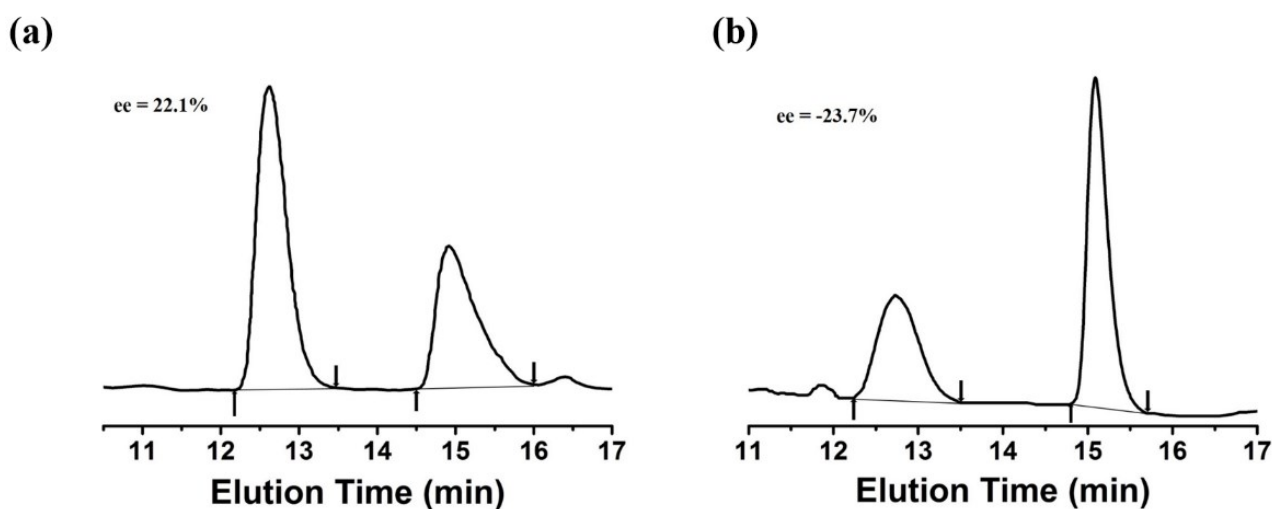


Figure S12. HPLC chromatograms of the residual reaction solution after (a) R-CPL and (b) L-CPL irradiation (containing unreacted 4-VPET monomer) with additional HAD.

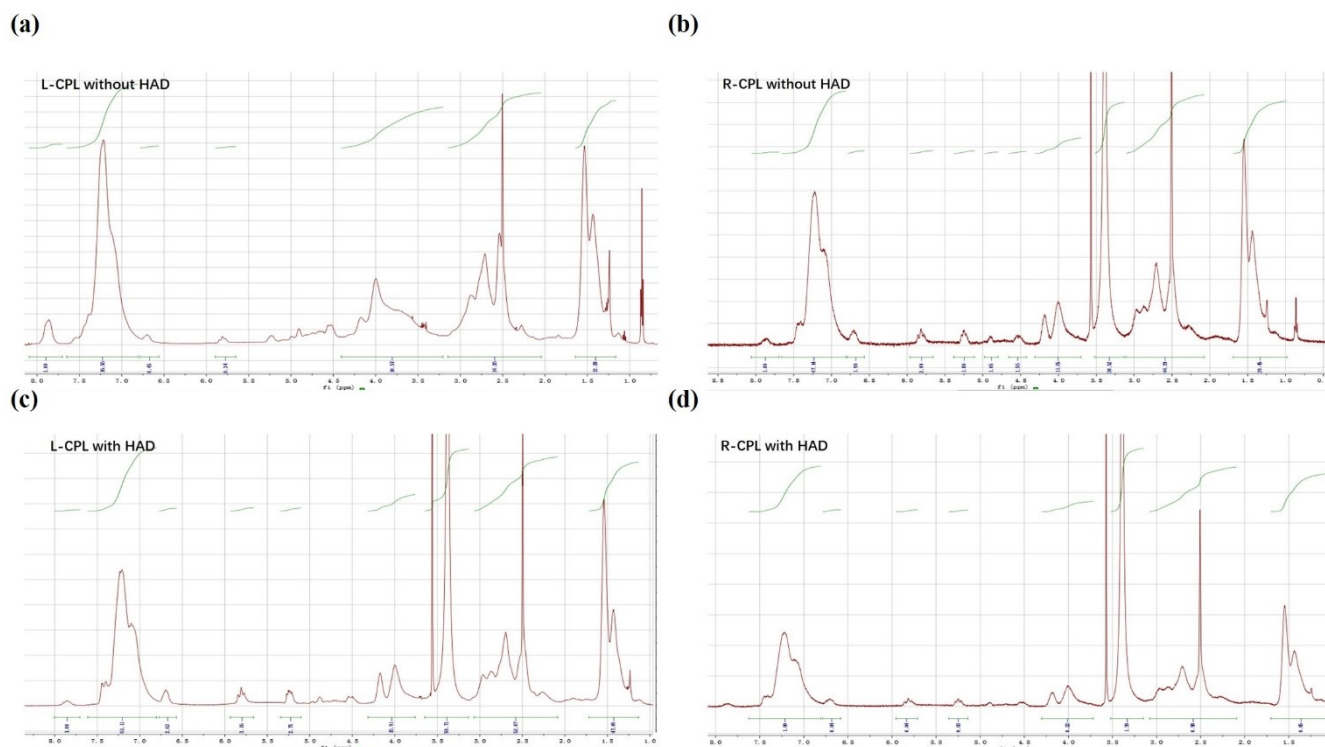


Fig. S13. ^1H NMR spectra of poly(thioether) irradiated by (a) L-CPL without HAD, (b) R-CPL without HAD, (c) L-CPL with HAD and (d) R-CPL with HAD.

Table S2. Monomer conversions and characterizations about poly(thioether).

Sample	Monomer conversion	Molar mass M_n	Molar weight M_w	Polymer dispersity index M_w/M_n
Upon L-CPL irradiation	72%	2941	5293	1.8
Upon R-CPL irradiation	69%	2874	4885	1.7
Upon L-CPL with HAD	59%	2057	4936	2.4
Upon R-CPL with HAD	63%	2356	5418	2.3

The M_n , M_w , and dispersity index determined by SEC using polystyrene for calibration.

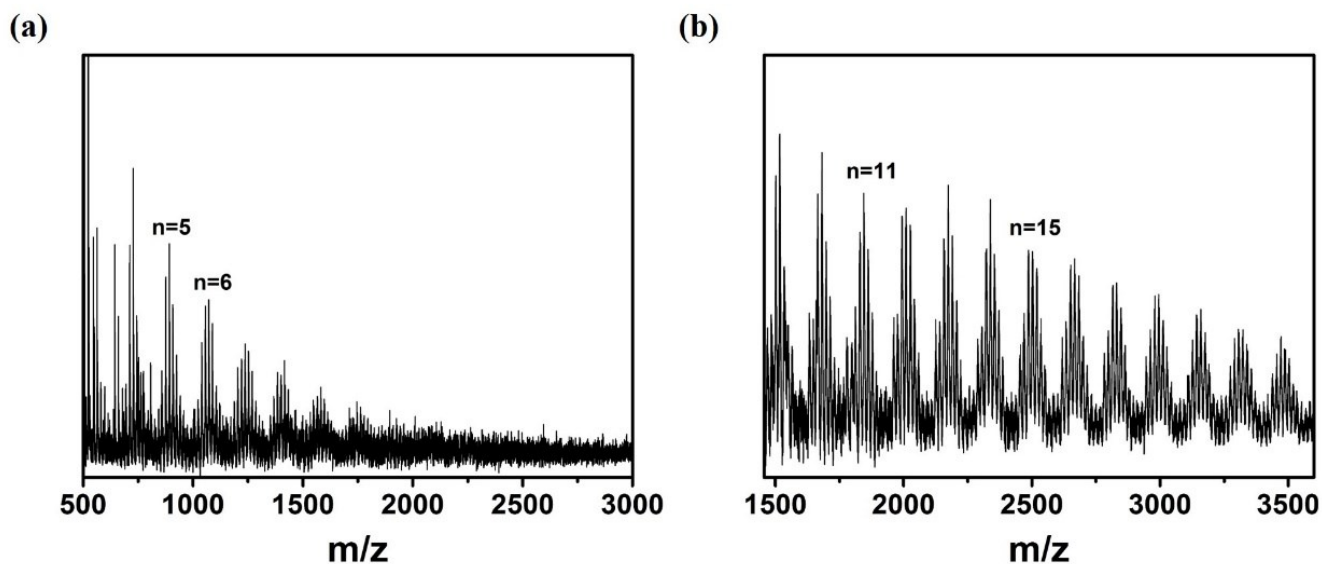


Fig. S14 Matrix-assisted laser desorption ionization time-of-flight mass (MALDI-TOF) spectra of poly(thioether) with (a) the lowest and (b) the highest mean molecular weight obtained from multiple fractions via successive centrifugal precipitation.

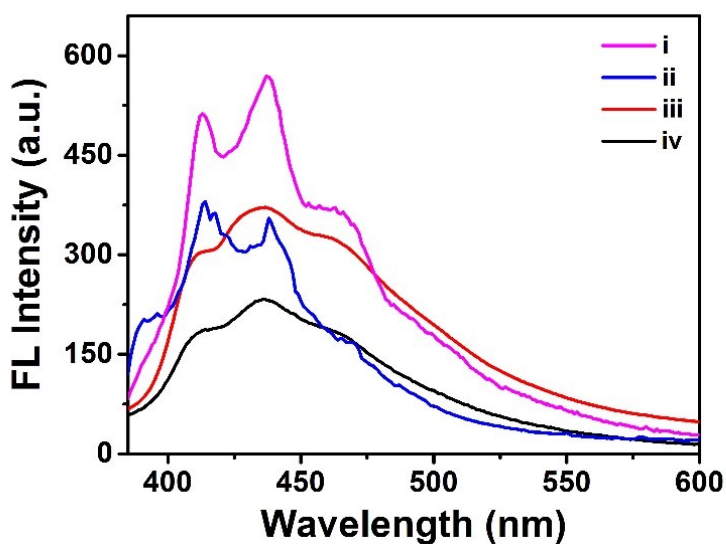


Figure S15. Luminescence of poly(thioether) (1.0 mg/mL) in (i) H₂O/THF (fw = 30%) at 77 K, (ii) THF at 77 K, (iii) H₂O/THF (fw = 30%) at 298 K and (iv) THF at 298 K, respectively.

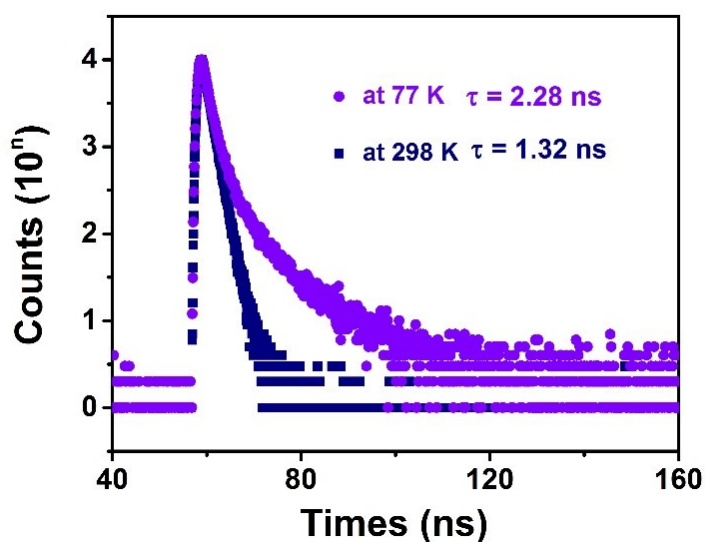


Figure S16. Luminescence lifetimes of poly(thioether) monitored at 435 nm in THF ($\lambda_{ex} = 330$ nm) at 77 K and 298 K, respectively.

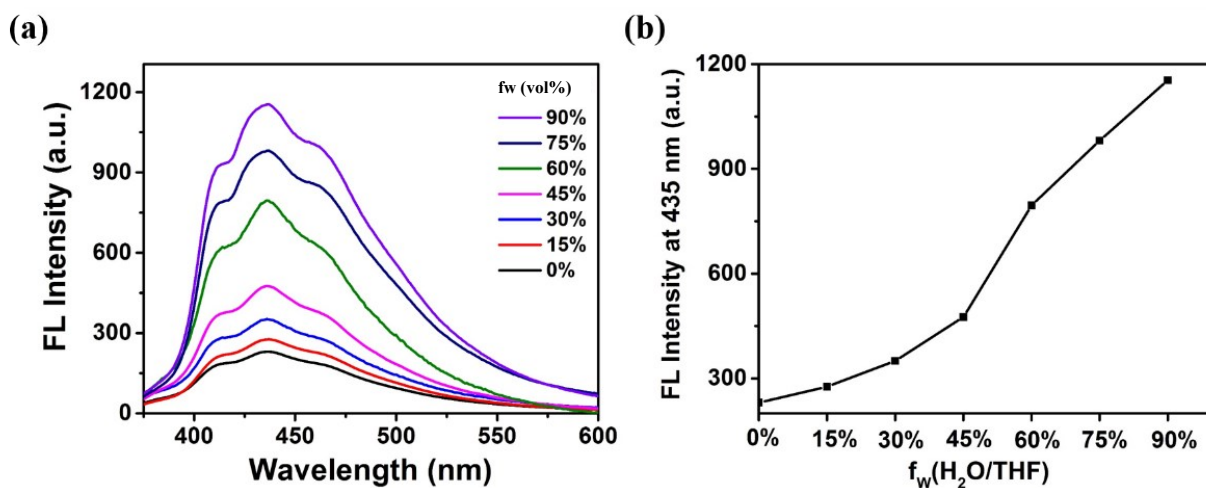


Figure S17. (a) Luminescence of poly(thioether) (1 mg/mL) in H₂O/THF mixtures at 298 K. Excitation: 330 nm. (b) Plot of the maximum luminescent intensity at 435 nm of poly(thioether) versus water fraction in H₂O/THF mixtures.

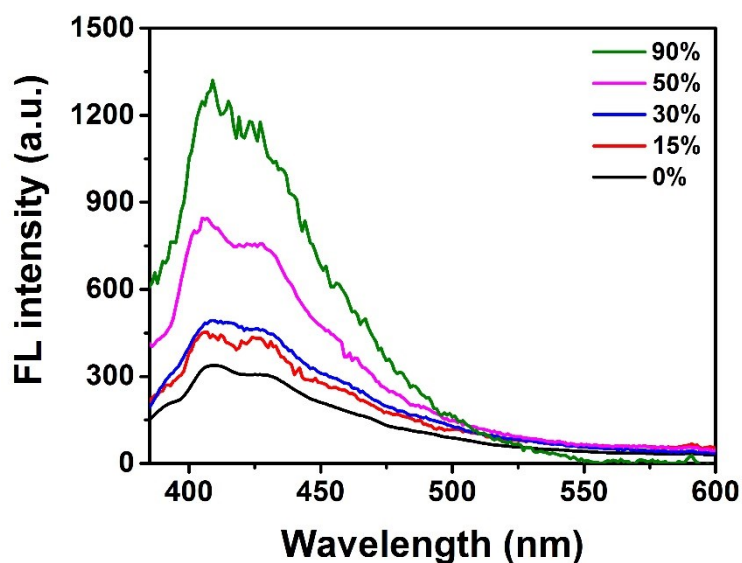


Figure S18. (a) Luminescence of poly(thioether) (1 mg/mL) in H₂O/THF mixtures at 77 K. Excitation: 330 nm.

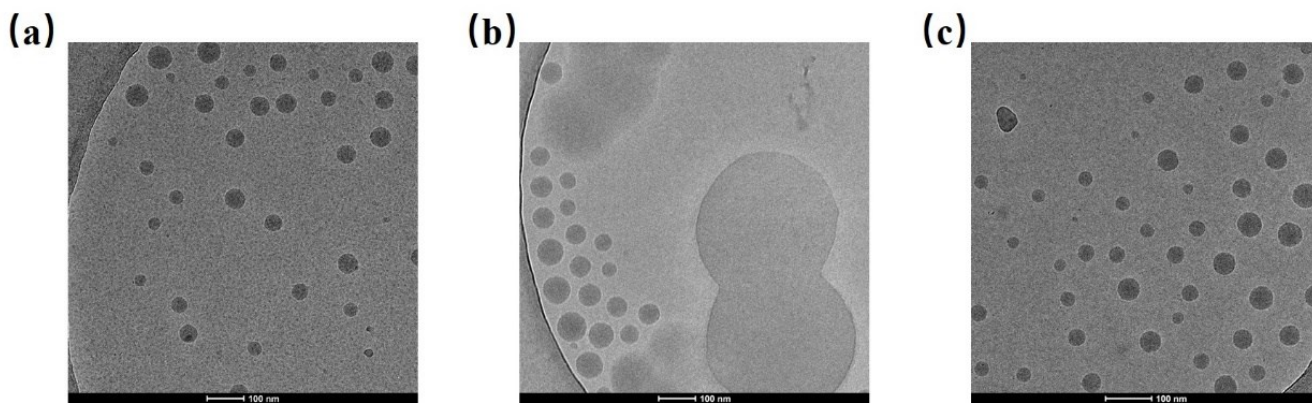


Figure S19. Cryo-electron microscopy images of poly(thioether) in (a) H₂O/THF (fw = 10%), (b) H₂O/THF (fw = 30%) and (c) H₂O/THF (fw = 90%) solution.

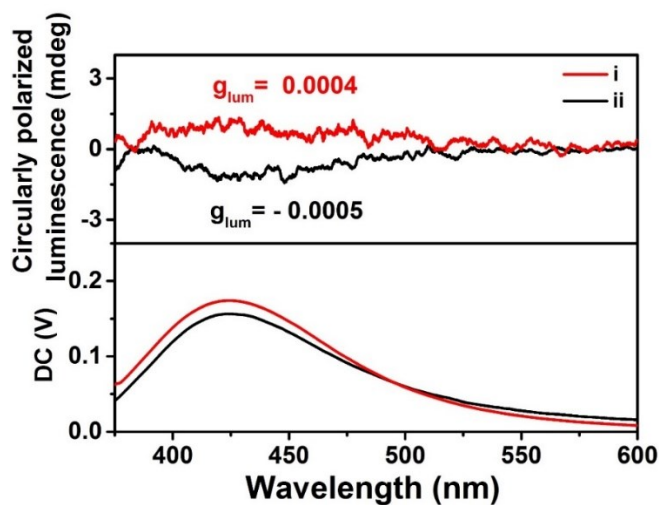


Figure S20. Circularly polarized luminescence spectra and corresponding g_{lum} factor of poly(thioether) prepared using (i) L-CPL and (ii) R-CPL without HAD. The data were taken in a 1.0 mg/mL H₂O/THF mixtures (fw = 30%) frozen at 77 K.

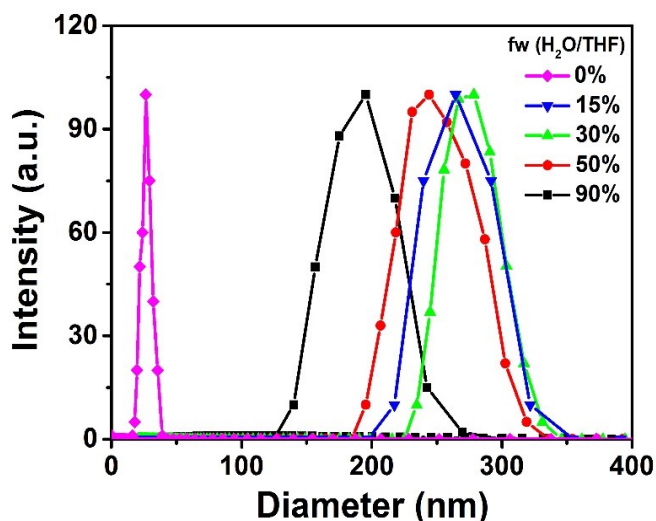


Figure S21. DLS curves of poly(thioether) measured in mixed H₂O and THF with different fractions of H₂O (fw).

Reference:

[1] A. Guerrero-Corella, A. M. Martinez-Gualda, F. Ahmadi, E. Ming, A. Fraile, J. Alemán, *Chem. Commun.* **2017**, 53, 10463-10466.